Dye-Sensitized Photocathodes: Boosting Photoelectrochemical Performances with Polyoxometalate Electron Transfer Mediators

Youssef Ben M'Barek, Timothy Rosser, Jérémy Sum, Sébastien Blanchard, Florence Volatron, Guillaume Izzet, Raphaël Salles, Jennifer Fize, Matthieu Koepf, Murielle Chavarot-Kerlidou, et al.

Dye-Sensitized Photocathodes: Boosting Photoelectrochemical Performances with Polyoxometalate Electron Transfer Mediators

Youssef Ben M'Barek,[†] Timothy Rosser,[‡] Jérémy Sum,[†] Sébastien Blanchard,[†] Florence Volatron,[†] Guillaume Izzet,[†] Raphaël Salles,[†] Jennifer Fize,[‡] Matthieu Koepf,[‡] Murielle Chavarot-Kerlidou,[‡] Vincent Artero,[‡] Anna Proust*[†]*

[†] Sorbonne Université, CNRS, Institut Parisien de Chimie Moléculaire, IPCM, 4 Place Jussieu, F-75005 Paris, France.

[‡] Univ. Grenoble Alpes, CNRS, CEA, IRIG, Laboratoire de Chimie et Biologie des Métaux, 17 rue des Martyrs, F-38000 Grenoble, France.

AUTHOR INFORMATION

Corresponding Authors

*E-mail:murielle.chavarot-kerlidou@cea.fr

*E-mail: anna.proust@sorbonne-universite.fr

ABSTRACT

The amplification effect of polyoxometalates (POMs) on the efficiency of dye-sensitized nano-ITO cathodes is disclosed. The use of hybrid polyoxometalates of the type $[PW_{11}O_{39}\{SnC_6H_4\text{-}{\equiv}\text{-}C_6H_4F\}]^{4-}$, F standing for a carboxylic group (**POM-COOH**) or a diazonium unit, allows to control the loading of the POMs on the electrode and to investigate key parameters. Even at very low loading, **POM-COOH** has a substantial effect on the photocurrent response, with up to 25-fold increase. Besides ensuring the stability towards leaching, the anchoring function of the POM hybrids was also found to play an intricate role in the competition between the multiple events involved.

Keywords: photocathodes, polyoxometalates, redox mediator, nano-ITO, photoelectrochemical cells

TOC GRAPHICS

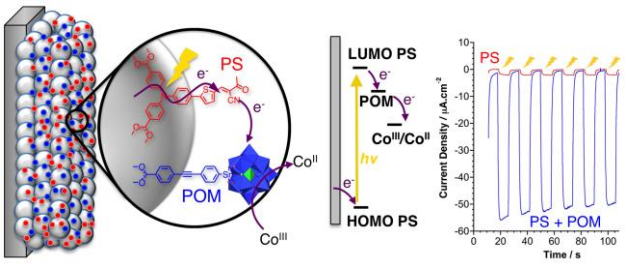

Depletion of fossil resources and environmental concerns make it urgent to increase renewable energies, namely solar energy, in the energy mix. However, these are intermittent by nature. To

overcome this shortcoming, the development of light-driven processes for water splitting as well as carbon dioxide reduction to produce fuels or raw chemicals is thoroughly investigated.[1] Implementation of these reactions requires the right choice of electrode substrates, light-harvesting units and catalysts, to avoid for example the use of platinum in the case of water electrolysis. Large-scale screening of catalysts, bulk materials or molecular species,[2-3] including their immobilization onto various inorganic materials and electrodes,[4-5] together with performance benchmarking[6-7] have been performed and reviewed. Still photo-electrochemical cells (PECs) are facing thermodynamic, kinetic and mass transfer limitations, which hinder the development of economically viable photosynthetic devices for solar fuel production.[8] Among the different approaches currently investigated to reach this goal, dye-sensitized photo-electrochemical cells (DSPECs) stem from the dye-sensitized solar cell (DSSC) technology and rely on the use of molecular catalysts and photosensitizers assembled on transparent semi-conducting oxide electrodes. While photo-anodes displaying important photocurrents, from a few hundreds of $\mu A.cm^{-2}$ to a few $mA.cm^{-2}$,[9-10] were reported, limitation in the development of functional DSPECs currently arises from the photocathode performances, which are often limited by the fast (<ns) rate of charge recombination at the oxide–dye interface.[11]

Electron transfer mediators such as Ru-polypyridyl complexes have been proposed to enhance the catalytic rate of the Oxygen Evolving Reaction (OER)[12] and to improve the stability of dye-sensitized photo-anodes by enabling rapid transfer of oxidative equivalents from the oxidized chromophore to the catalyst.[13] This prompted us to assess the ability of polyoxometalates (POMs) as electron transfer (or redox) mediators to boost the activity of dye-sensitized photocathodes in aqueous solution, *i.e.* relevant to technological PEC applications.

POMs are molecular oxides of the early transition metals in their highest oxidation states of the general formula $[X_xM_pO_y]^{n-}$ (X= P, Si …; M = Mo^{VI}, W^{VI}, V^{V}…) and endowed with outstanding redox properties: they can be successively and reversibly reduced with minimal structural reorganization. They have already been used as redox mediators in light-driven Z-scheme water splitting[14] and as both electron/proton reservoirs and shuttles in CO_2 reduction reaction (CO_2RR) operated by an hybrid POM-rhenium complex catalyst.[15-16] The inorganic POM scaffolds can be functionalized with an organic extension to generate POM hybrids.[17] These compounds can display remote active sites for extra transition metal coordination, assembly in advanced architectures or covalent anchorage onto substrates.[18] Some of us have been deeply engaged in the synthesis and implementation of POM hybrids and we have recently described the immobilization of $[PW_{11}O_{39}\{SnC_6H_4\text{-}\equiv\text{-}C_6H_4COOH\}]^{4-}$ (**POM-COOH**) onto Si/SiO_2 wafers,[19] and the grafting of $[PM_{11}O_{39}\{M'C_6H_4\text{-}\equiv\text{-}C_6H_4\text{-}N_2^+\}]^{3-}$ (M = W, Mo, M'= Ge, Sn) on various electrodes, including glassy carbon, graphene and silicon.[20-21] We herein report the amplification effect of a co-grafted POM on the photo-electrochemical activity of a dye-sensitized photocathode.

Elaboration of the photocathodes

We have chosen a covalent bottom-up strategy for its modularity and control over the design of the electrode. Nanostructured mesoporous ITO films (nano-ITO) have been functionalized by co-grafting a benchmark push-pull organic dye and either **POM-COOH** or $[PW_{11}O_{39}\{SnC_6H_4\text{-}\equiv\text{-}C_6H_4\text{-}N_2^+\}]^{3-}$ (**POM-diazo**), allowing to test the influence of the POM anchoring group. The push-pull dye 4,40-((4-(5-(2-cyano-3-ethoxy-3-oxoprop-1-en-1-yl)thiophen-2-yl)phenyl)azanediyl)dibenzoic acid combines a triarylamine electron donor and a cyanoacetate

electron acceptor and also displays carboxylic acid functions for grafting onto the oxide substrate (see Figure 1). It has been successfully integrated by some of us in NiO-based photocathodes for HER and will be referred to as the photosensitizer (**PS**).[22-24]

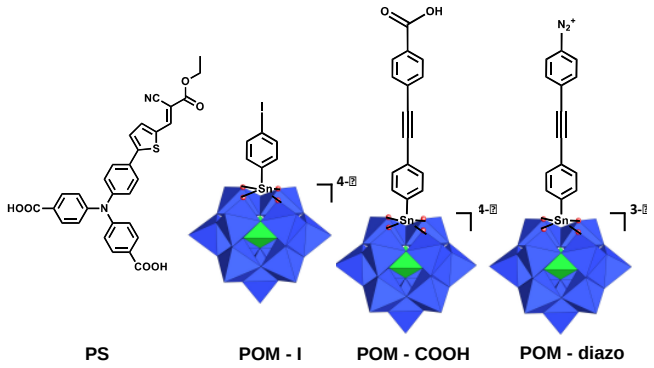

Figure 1. From left to right, drawing of the push-pull organic dye and polyhedral representation of $[PW_{11}O_{39}\{SnC_6H_4I\}]^{4-}$ (**POM-I**), $[PW_{11}O_{39}\{SnC_6H_4$-≡-$C_6H_4COOH\}]^{4-}$ (**POM-COOH**) and $[PW_{11}O_{39}\{SnC_6H_4$-≡-C_6H_4-$N_2^+\}]^{3-}$ (**POM-diazo**); the WO_6 octahedra are depicted with oxygen atoms at the vertices and metal cations buried inside. Color code: WO_6 octahedra, blue; PO_4 tetrahedra, green.

The preparation of the nano-ITO films has been adapted from a procedure previously reported for tin oxide (SnO_2) films (see SI).[25] A film thickness of 640-650 nm was measured by optical interferometry. For the co-grafting of **PS** and **POM-COOH**, the nano-ITO substrate was dipped for 24 h into an acetonitrile (ACN) solution containing **PS** and **POM-COOH** in given concentrations, then rinsed with ACN and dried in air. Sonication was avoided in order to preserve the mechanical integrity of the nanostructured films. The dye-sensitized electrodes will be labeled according to the PS:POM co-loading ratio, which does not reflect the ratio in the grafted species (see below and Table 1). We have thus prepared the following substrates 1PS:1POM (dipping solution 0.5 mM in **PS** and 0.5 mM in **POM-COOH**), 1PS:2POM (dipping solution 0.5 mM in **PS** and 1 mM in **POM-COOH**), and 1PS:5POM (dipping solution 0.5 mM in **PS** and 2.5 mM in **POM-COOH**), which was compared to 0.2 PS:1POM (dipping solution

0.1 mM in PS and 0.5 mM in **POM-COOH**). Blank substrates were also prepared by soaking in solution of pure **PS** or pure **POM-COOH** (0.5 mM).

The co-grafting of the **POM-diazo** and **PS** was carried out in two successive steps: in the first step, $[PW_{11}O_{39}\{SnC_6H_4\text{-}\equiv\text{-}C_6H_4\text{-}N_2^+\}]^{3-}$ was generated in situ by adding an excess of $^tBuNO_2$ to a 1 mM solution of $(n\text{-}Bu_4N)_4[PW_{11}O_{39}\{SnC_6H_4\text{-}\equiv\text{-}C_6H_4\text{-}NH_2\}]$ in ACN and placed in an electrochemical cell. Covalent grafting onto the nano-ITO film was then performed through electroreduction of the diazonium function, the nano-ITO electrode being used as the working electrode. The electrochemical reduction of the diazonium group generates a radical upon N_2 release, which couples to the electrode to form a strong covalent bond. In a second step, the POM-modified electrode was soaked in a 0.5 mM solution of **PS** in ACN, as previously described and finally rinsed and dried in air.

The same procedure (1PS:1POM) was also applied with the parent POM hybrid $[Pw_{11}O_{39}\{SnC_6H_4I\}]^{3-}$ (**POM-I**), which is the precursor in the synthetic pathway to both **POM-COOH** and **POM-diazo** but does not have any anchoring group. After the rinsing step **POM-I** is not expected to be immobilized on the substrate.

Characterization of the photocathodes

Surface coverage has been assessed by various techniques. Electronic absorption spectroscopy is the most convenient for the organic dye, which is characterized in ACN solution by a charge transfer band at 436 nm with an extinction coefficient ε_{max} = 29 300 M^{-1} cm^{-1}.[22] After grafting, a slight red-shift is observed and the maximum of absorbance (A_{max}) has been measured at 450 nm, after subtraction of the spectrum of the bare nano-ITO recorded for each slide before

sensitization (see Figure S1). The surface loading (reported versus the geometrical surface area of the electrode) was then calculated for the various substrates using the following equation:[26]

$$\Gamma\ (mol.cm^{-2}) = \frac{A_{max}}{1000\ \times\ \varepsilon_{max}\ (L.mol^{-1}.cm^{-1})}$$

In the case of the **PS**/**POM-COOH** substrates, the dye loading was found to be remarkably constant from one sample to the other (see histogram in Figure S2), even when using a dipping solution of only 0.2 mM in **PS**. The average value of 1.1×10^{-8} mol cm^{-2} is fully consistent with the values previously reported on another structured nickel oxide electrodes. [22, 24] (Note that this value is overestimated when compared to grafting onto planar substrates because it does not take into account the real oxide surface available.) For the **PS/POM-diazo** modified electrodes, the dye loading determined by UV-Vis measurements is again similar. Although POMs are characterized by strong ligand to metal charge transfer bands in the UV range, this did not enable the evaluation of their loading because of the important absorption of ITO in this range.

Yet wavelength dispersive spectroscopy (WDS), a sensitive technique to perform compositional analysis of the surface, allowed for the quantification of the POM loading. A mapping of S and W atoms, representative of the dye and the POM respectively, is displayed in Figure 2 and the atomic percentages are given in Table 1 for various slides. Several conclusions have been drawn from these data: i) Both the dye and the POM coverages are uniform. ii) In any case, the dye loading is much higher than that of the POM with a PS/POM ratio ranging from 141 (1PS:1POM slide) to 14 (0.2PS:1POM); This is consistent with the XPS characterization of a 1PS:1POM substrate (see Figure S7) which gives a ratio of S over W integrated peaks of 9.4 *i.e.* a PS/POM ratio of 104; iii) Among the **PS/POM-COOH** modified substrates, the variation

of the S atomic percentage is small from one substrate to another, in agreement with the conclusion drawn from the UV-vis characterization. Conversely, the W atomic percentage depends more on the initial PS/POM concentration ratio in the dipping solution, the lower the ratio the higher the POM loading, albeit much lower than that of the PS (sometime at the limit of detection). Note also that similar values have been obtained for 1PS:5POM and 0.2PS:1POM, suggesting that the initial concentrations can be reduced without affecting the efficiency of the grafting.

In the case of the **PS/POM-diazo** substrate, a PS/POM ratio of 21 is obtained, comparable to that of 1PS:5POM **PS/POM-COOH** substrates. Finally, whereas the WDS analysis of the **PS/POM-**I electrode confirmed the presence of the dye, the concentration of W on the surface is, as expected below the limit of detection. The rinsing step of the grafting protocol probably leads to the leaching of the physisorbed **POM-I**.

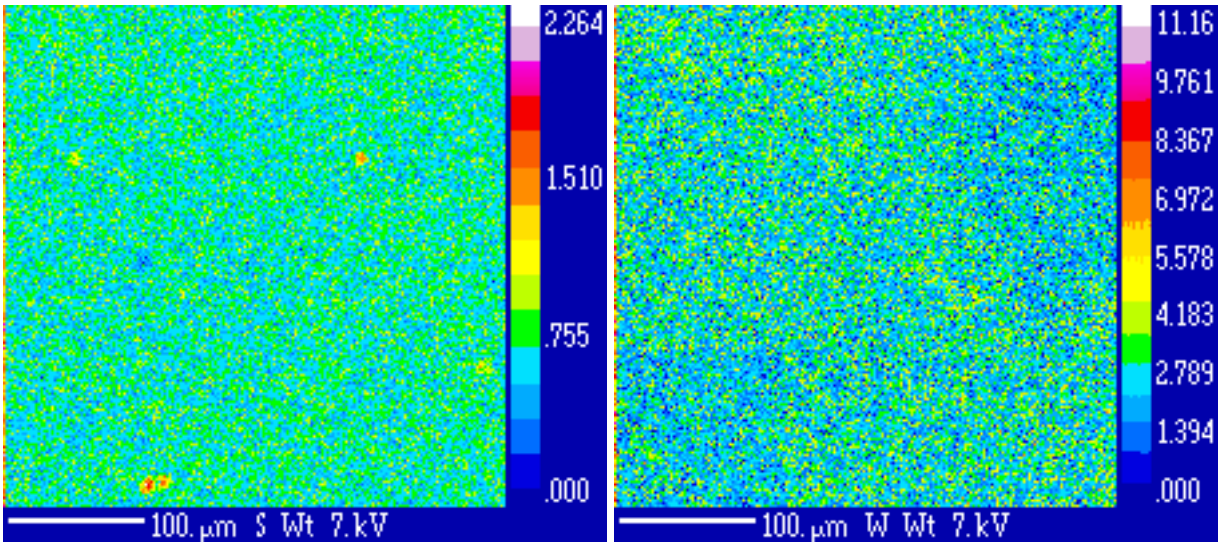

Figure 2. Mapping of the S (left) and W (right) loading by Wavelength Dispersion Spectroscopy analysis on 1PS:2POM substrate.

Table 1. Wavelength Dispersion Spectroscopy analysis of different PS/POM loading substrates

	S atomic %	Standard deviation	W atomic %	Standard deviation	PS/POM ratio
1PS:1POM	0.51	0.05	0.04	0.06	141
1PS:2POM	0.47	0.05	0.06	0.05	81
1PS:5POM	0.63	0.05	0.40	0.06	16
0.2PS:1POM	0.49	0.06	0.35	0.06	14
PS + POM-I	0.55	0.06	-	-	-
PS:POM-diazo	0.41	0.05	0.19	0.06	21

Finally, we turned to electrochemistry, which is usually a prime technique to characterize and quantify the presence of POMs. The cyclic voltammogram of **POM-COOH**, recorded in ACN solution at a glassy carbon electrode, is characterized by two quasi-reversible well-defined reduction processes at -1.11 and -1.57 V *vs* Ag/AgCl. In general, these waves can be used to assess the POM density on the electrode after immobilization.[20] Indeed, the cyclic-voltammogram recorded at a nano-ITO slide modified with the **POM-diazo** and used as a working electrode (before dye incorporation) in a pure electrolyte solution discloses the expected POM-reduction waves at -1.08 and -1.48 V *vs* Ag/AgCl (see Figure S4) and a POM packing density of 1.35×10^{-10} mol cm^{-2} was obtained by integration of the first wave. Given the porous nature of the electrode, this value corresponds to a sub-monolayer and thus pre-grafting of the POM should not hinder the immobilization of the dye, realized in subsequent step, as discussed above for the UV-Vis characterization.

Surprisingly, using the **POM-COOH** nano-ITO modified substrates (with or without **PS**) as the working electrode we observed only an ill-defined irreversible wave, whatever the scan rate, from 10 to 500 mV s^{-1} (see Figure S5). Changing the anchoring function on the surface thus turned out to lead to kinetically inhibited electron transfer and thus did not allow for quantitative

measurement of the POM on the surface. Interestingly, these experiments demonstrate how the nature of the grafting mode influences the electronic communication between the nano-ITO substrate and the grafted POMs.

Photocurrent assessment

The as-modified nano-ITO slides have been evaluated as photocathodes (active area 0.5 cm^2) in a three electrode cell configuration comprising a Pt counter electrode, a Ag/AgCl (KCl saturated) reference electrode and $[Co(NH_3)_5Cl]Cl_2$ as an irreversible electron acceptor, 1 mM in a pH 3.75 acetic buffer (0.1 M).[22] The pH value was set at the stability limit of the parent $K_4[PW_{11}O_{39}\{SnC_6H_4I\}]$ as monitored by ^{31}P NMR. Measurements were performed at ~1 sun. According to the linear sweep voltammograms (LSV, 100 mV s^{-1}) first recorded for a PS-electrode (photocathode containing only the dye, see Figure S8) and then a 1PS:1POM electrode (see Figure 3), the working potential was fixed at +0.3 V *vs* Ag/AgCl for the subsequent photocurrent measurements. We also verified that in these conditions the POM-electrode (photocathode with POM only) is not photoactive (see LSV in Figure S8).

Comparison of the photocurrent densities recorded for the **PS**-electrode and the 1PS:1POM electrode is displayed in Figure 3, which demonstrates the promoting effect of the POM, with more than a 10-fold increase of the plateau value from -1.9 $\mu A.cm^{-2}$ to -23.8 $\mu A.cm^{-2}$. The photocurrents were shown to be stable from one measurement to another carried out several weeks apart (see Figure S10). For a given electrode, we have also verified that there is no change in the photocurrent density upon multiple renewal of the cobalt solution (see Figure S11). This absence of leaching is to be attributed to the covalent grafting of both the dye and the POM and a guarantee of robustness of the system. The electrode is thus reusable, under the same or variable

conditions, thus avoiding overconsumption of the active molecules. A possible explanation about the role of the POM relies on an energy level alignment with transient reduction of the POM as sketched in Scheme 1.

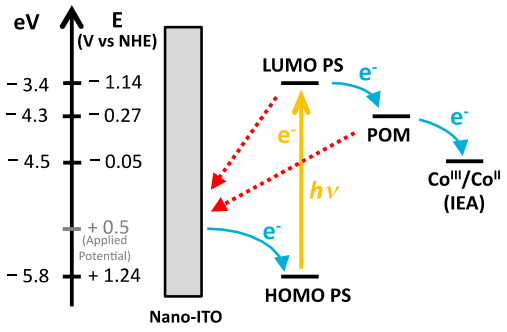

Scheme 1. Proposed energy level diagram showing electron transfer processes thermodynamically possible after irradiation in the presence of the irreversible electron acceptor (IEA) and possible recombination paths (in red). The redox potential of the POMs in aqueous solution has been derived from the cyclic voltammogram of **POM-I** (rubidium salt) (see Figure S6 the redox potential is independent of the terminal group on the POM hybrid see reference 31);

As electronic absorption spectra of reduced POMs are characterized by broad intervalence charge transfer (IVCT) bands in the visible, it has been suggested that reduced POMs can be used as photosensitizers.[16, 27] A bandpass filter (centered around 450 nm, 50 nm width) has thus been fixed on the optical bench to prevent their excitation. This filter still allows for the excitation of the dye, as we have indeed verified with the **PS**-electrode. A 45% lowering of the photo-current was observed probably due to some absorption by the filter itself and reduction of the irradiation power. A similar lowering (58%), was observed for the 1PS:1POM electrode,

ruling out the involvement of an IVCT event in our case (see Figures S12 and S13).

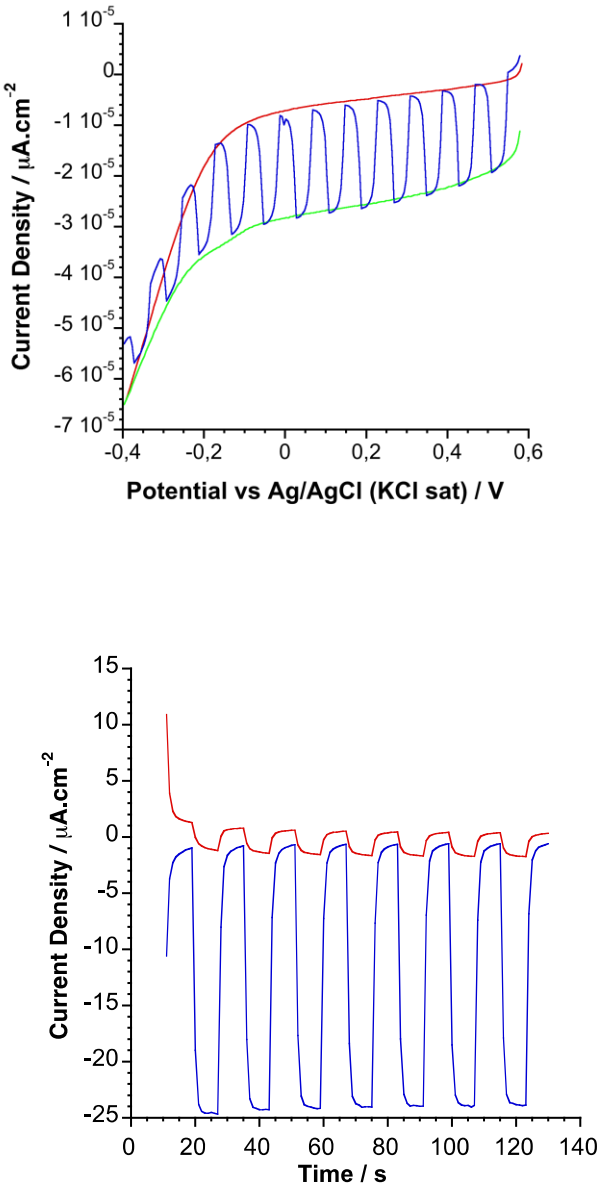

Figure 3. Top : linear sweep voltammogram (100 $mV.s^{-1}$) recorded in the dark (red), under light (green) and under chopped light (blue), on the 1PS :1POM **PS/POM-COOH** nano-ITO substrate in $[Co(NH_3)_5Cl]Cl_2$ 1 mM in pH 3.75 acetate buffer (0.1 M); bottom: cathodic photocurrents recorded at +0.3 V vsAg/AgCl applied potential (blue) compared to those recorded on the **PS**-electrode (red).

Since the trend in the **POM-COOH** loading follows its initial concentration in the soaking solution, we have investigated its effect on the intensities of the photocurrents. The loading of the dye being conversely almost unchanged, direct correlations are then possible. Variability from one substrate to the other is a common shortcoming in surface chemistry so each experiment has been repeated at least on two different slides, taken from the same batch and modified concomitantly by soaking into the same solution. The results obtained for various 1PS:nPOM ratios and 0.2PS:1POM are presented in Figure 4. The increase of the photocurrent densities does not vary linearly with the POM loading, the most intense photocurrent density being obtained with the 1PS:2POM ratio(50 $\mu A.cm^{-2}$), which corresponds to a 25-fold gain in current density. To more accurately assess the ability of the grafted photosensitizer to mediate electron transfer from the nano-ITO film to the final irreversible electron acceptor (IEA) in the different electrode constructions, the photocurrent density was reported versus the surface concentration in **PS** (determined for each film prior to the measurement). This further allowed to estimate a macroscopic electron transfer rate, expressed as the amount of reduced IEA per **PS** and per second (Table 2). The 25-fold increase for the 1PS:2POM photocathode could result from a fine balance between all the events occurring at the photoelectrode/electrolyte interface, electron transfer from the photo-excited dye (oxidative quenching mechanism) or reduced dye (generated upon hole injection from the dye excited state into the conduction band of nano-ITO) to the POM and from the reduced POM to the cobalt acceptor, notwithstanding the less efficient electron transfer from the excited/reduced dye to the cobalt complex, but also multiple recombination pathways (Scheme 1). This could also be due to a better confinement of the cationic cobalt complex at the vicinity of the surface through electrostatic interactions with the POM. Because of the interplay of competition between these multiple events, improving the

performance of photo-electrodes is complex: in a recent example Lindqvist-type POMs used as coadsorbents in p-type NiO-based Dye Sensitized Solar Cell (p-DSSC) were found to impede both back recombination to NiO and electron transfer to the electrolyte thus resulting in a poor effect on the overall efficiency.[28] More generally, the photocurrents that have been recorded in other POM-based systems like DSCCs are at least one order of magnitude lower that those reported in this work.[29-30]

The 1PS:5POM and 0.2PS:1POM electrodes behave quite similarly: this is in agreement with the UV-vis analysis, which suggested a similar dye loading, and the WDS analysis, which gave quite comparable W/S ratio. This should, in the future, allow scaling down the active species.

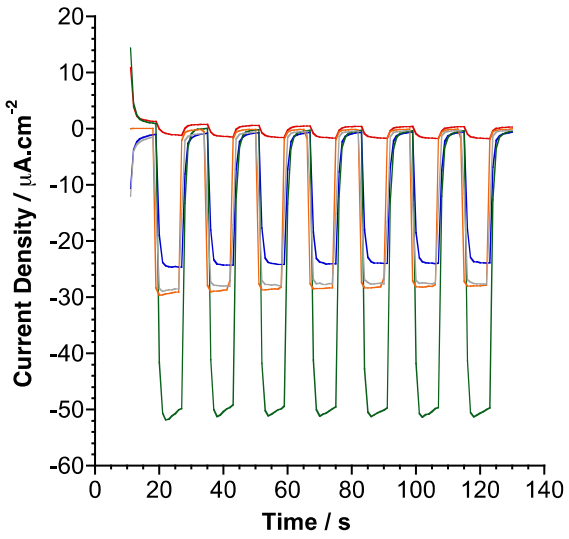

Figure 4. Cathodic photocurrents recorded on 1PS:1POM (blue),1PS:2POM (green), 1PS:5POM (orange) and 0.2PS:1POM (grey) **PS/POM-COOH** nano-ITO electrode in $[Co(NH_3)_5Cl]Cl_2$ 1 mM in pH 3.75 acetate buffer (0.1 M) at + 0.3 V vs Ag/AgCl applied potential, compared to those obtained on the **PS**-electrode (red).

Table 2. Cathodic photocurrent density and macroscopic electron transfer rate of the electron transfer to the cobalt complex related to the POM:PS ratios.

	Photocurrent density ($\mu A.cm^{-2}$)	Cathodic photocurrent density per nmol of grafted photosensitizer[a] ($\mu A.nmol^{-1}$)	Macroscopic electron transfer rate ($mol(reduced\ IEA).mol(PS)^{-1}.\ s^{-1}$)[b]
PS	1.9	0.18	0.002
1PS:1POM	23.8	1.90	0.020
1PS:2POM	50.0	4.31	0.045
1PS:5POM	28.5	2.54	0.026

[a]Calculated with the mean PS density of each substrate. [b]Considering 1 A = 1 $C.s^{-1}$ and 1 Faraday = 96500 C.

To stress the importance of the anchoring group of the POM hybrid, we have undertaken the same study with the **PS/POM-diazo** and **PS/POM-I** photocathodes. Figure 5 presents the photocurrents measurements for both modified electrodes. For the **PS/POM-I** electrode, the photocurrent density is very similar to that of the PS-electrode, probably due to the very low loading of physisorbed POM as mentioned above. This also rules out an electrostatic deposition of **POM-COOH**. In the case of the **PS/POM-diazo** photocathode, surprisingly, the photocurrent enhancement is considerably lower than that observed **with POM-COOH** while according to the WDS analysis, the PS/POM ratio is similar to the one obtained for 1PS:5POM. A tentative explanation is that the good electronic communication between the nano-ITO and the POM as revealed by CV also fosters electron back recombination at the expense of electron transfer to the cobalt acceptor. This also underscores that the electrostatic interaction between the polyanion and the cationic cobalt complex used as an irreversible electron acceptor is not the major factor explaining the enhancement of the photocurrents.

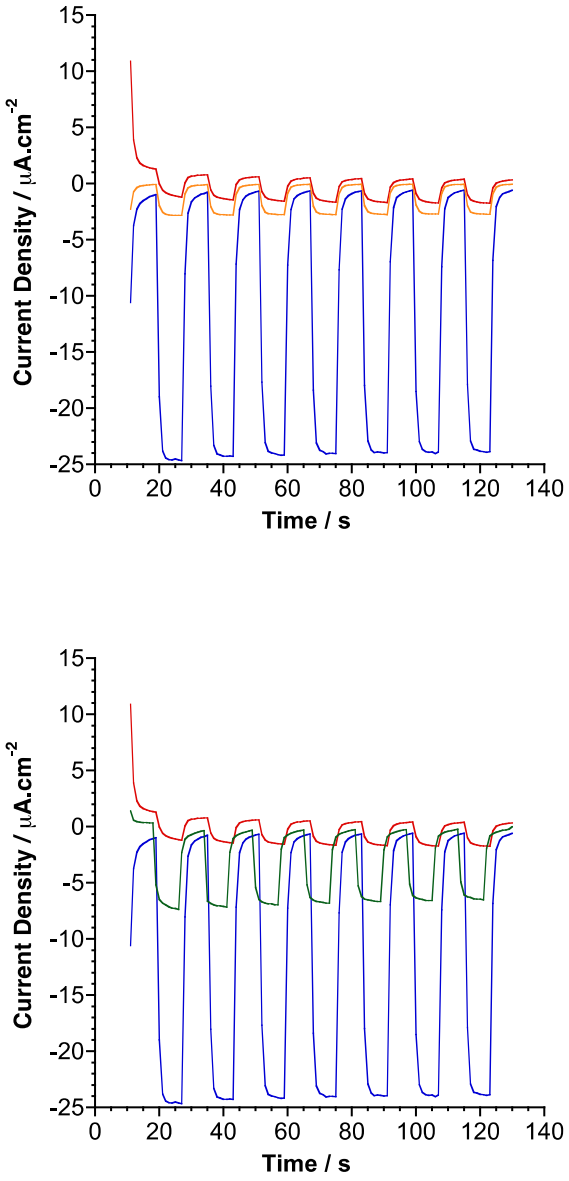

Figure 5. Cathodic photocurrents recorded in $[Co(NH_3)_5Cl]Cl_2$ 1 mM in pH 3.75 acetate buffer (0.1 M) at 0.3 V vs Ag/AgCl applied potential Top: with a nano-ITO electrode prepared by soaking in an equimolar 0.5 mM solution of the **PS** and **POM-I** in ACN (orange); bottom: with a nano-ITO electrode prepared by electrografting of $[PW_{11}O_{39}\{SnC_6H_4\text{-}\equiv\text{-}C_6H_4\text{-}N_2^+\}]^{3-}$ and subsequent soaking in a 0.5 mM solution of the **PS** (green). Both are compared to the photocurrents obtained on a 1PS:1POM **PS/POM-COOH** nano-ITO electrode (blue) and to those obtained on the **PS**-electrode (red).

Conclusion

Nanostructured mesoporous ITO films (nano-ITO) have been functionalized by the co-grafting of a push-pull organic photosensitizer and hybrid POMs in various ratios. Thorough characterization by UV-Vis spectroscopy, wavelength dispersive spectroscopy, XPS and electrochemistry confirmed the presence and integrity of both components, that they are uniformly dispersed on the substrate and provided cross-evaluation of their respective loading. Whereas the loading of the dye has been found to be remarkably constant, variation of the concentration of the hybrid POM in the initial soaking solution allowed to tune the final amount of POMs on the substrate. In any case the POMs grafting is much lower than that of the dye. However, even at this very low loading ratio, **POM-COOH** co-grafting results in a substantial enhancement(up to a factor of 25) of the photocurrent response of the as prepared photocathodes in aqueous solution. A detailed understanding of the electron transfer dynamics at the nano-ITO interface will be required in the future to better apprehend the beneficial role played by the POM unit. Furthermore, we show that the nature of the anchoring function of the POM and its loading are keys parameters to optimize the performance of the resulting photocathodes. Future work will exploit this key finding to design active photocathodes for H_2 production and CO_2 reduction though their combination with suitable multi-electron multi-proton catalysts.

ASSOCIATED CONTENT

Supporting Information Materials and general procedures; physical measurements; monitoring of the dye grafting by UV-visible spectroscopy; electrografting of [$PW_{11}O_{39}${SnC_6H_4-≡-C_6H_4-

$N_2^+\}]^{3-}$ onto nano-ITO; vain assesment of the **POM-COOH** grafting by electrochemistry; POM electrochemical signature in acetic buffer; XPS characterization of the 1PS :1POM electrode; photocurrents measurements; SEM of the 1PS:1POM **PS**/**POM-COOH** nano-ITO film

AUTHOR INFORMATION

Corresponding Authors

*E-mail:murielle.chavarot-kerlidou@cea.fr

*E-mail: anna.proust@sorbonne-universite.fr

ACKNOWLEDGMENTS

This work was also supported by the French National Research Agency within grant ANR PhotoCarb (ANR-16-CE05-0025-03), the Labex program ARCANE (ANR-11-LABX-0003-01) and CBH-EUR-GS (ANR-17-EURE-0003). The authors warmly thank Christel Laberty-Robert from the Laboratoire de Chimie de la Matière Condensée de Paris for the privileged access to her photo-electrochemical set-up.

REFERENCES

(1) Ardo, S.; Rivas, D. F.; Modestino, M. A.; Greiving, V. S.; Abdi, F. F.; Alarcon Llado, E.; Artero, V.; Ayers, K.; Battaglia, C.; Becker, J. P.; Bederak, D.; Berger, A.; Buda, F.; Chinello, E.; Dam, B.; Di Palma, V.; Edvinsson, T.; Fujii, K.; Gardeniers, H.; Geerlings, H.; Hashemi, S. M. H.; Haussener, S.; Houle, F.; Huskens, J.; James, B. D.; Konrad, K.; Kudo, A.; Kunturu, P. P.; Lohse, D.; Mei, B.; Miller, E. L.; Moore, G. F.; Muller, J.;

Orchard, K. L.; Rosser, T. E.; Saadi, F. H.; Schuttauf, J. W.; Seger, B.; Sheehan, S. W.; Smith, W. A.; Spurgeon, J.; Tang, M. H.; van de Krol, R.; Vesborg, P. C. K.; Westerik, P., Pathways to Electrochemical Solar-Hydrogen Technologies. *Energy Environ. Sci.* **2018,** *11*, 2768-2783.

(2) Takeda, H.; Cometto, C.; Ishitani, O.; Robert, M., Electrons, Photons, Protons and Earth-Abundant Metal Complexes for Molecular Catalysis of CO_2 Reduction. *ACS Catal.* **2017,** *7*, 70-88.

(3) Zhang, B. B.; Sun, L. C., Artificial Photosynthesis: Opportunities and Challenges of Molecular Catalysts. *Chem. Soc. Rev.* **2019,** *48*, 2216-2264.

(4) Queyriaux, N.; Kaeffer, N.; Morozan, A.; Chavarot-Kerlidou, M.; Artero, V., Molecular Cathode and Photocathode Materials for Hydrogen Evolution in Photoelectrochemical Devices. *J. Photochem. Photobiol., C* **2015,** *25*, 90-105.

(5) Dalle, K. E.; Warnan, J.; Leung, J. J.; Reuillard, B.; Karmel, I. S.; Reisner, E., Electro- and Solar-Driven Fuel Synthesis with First Row Transition Metal Complexes. *Chem. Rev.* **2019,** *119*, 2752-2875.

(6) Costentin, C.; Robert, M.; Saveant, J. M., Current Issues in Molecular Catalysis Illustrated by Iron Porphyrins as Catalysts of the CO2-to-CO Electrochemical Conversion. *Acc. Chem. Res.* **2015,** *48*, 2996-3006.

(7) McCrory, C. C. L.; Jung, S.; Ferrer, I. M.; Chatman, S. M.; Peters, J. C.; Jaramillo, T. F., Benchmarking Hydrogen Evolving Reaction and Oxygen Evolving Reaction Electrocatalysts for Solar Water Splitting Devices. *J. Am. Chem. Soc.* **2015,** *137*, 4347-4357.

(8) Larrazabal, G. O.; Martin, A. J.; Perez-Ramirez, J., Building Blocks for High Performance in Electrocatalytic CO_2 Reduction: Materials, Optimization Strategies, and Device Engineering. *J. Phys. Chem. Lett.* **2017,** *8*, 3933-3944.

(9) Yu, Z.; Li, F.; Sun, L. C., Recent Advances in Dye-Sensitized Photoelectrochemical Cells for Solar Hydrogen Production Based on Molecular Components. *Energy Environ Sci.* **2015,** *8*, 760-775.

(10) Xu, P. T.; McCool, N. S.; Mallouk, T. E., Water Splitting Dye-Densitized Solar Cells. *Nano Today* **2017,** *14*, 42-58.

(11) Gibson, E. A., Dye-Sensitized Photocathodes for H_2 Evolution. *Chem. Soc. Rev.* **2017,** *46*, 6194-6209.

(12) Concepcion, J. J.; Jurss, J. W.; Templeton, J. L.; Meyer, T. J., Mediator-Assisted Water Oxidation by the Ruthenium "Blue Dimer" cis,cis-$[(bpy)_2(H_2O)RuORu(OH_2)(bpy)_2]^{4+}$. *Proc. Natl. Acad. Sci. U. S. A.* **2008,** *105*, 17632-17635.

(13) Wang, D. G.; Eberhart, M. S.; Sheridan, M. V.; Hu, K.; Sherman, B. D.; Nayak, A.; Wang, Y.; Marquard, S. L.; Dares, C. J.; Meyer, T. J., Stabilized Photoanodes for Water Oxidation by Integration of Organic Dyes, Water Oxidation Catalysts, and Electron-Transfer Mediators. *Proc. Natl. Acad. Sci. U. S. A.* **2018,** *115*, 8523-8528.

(14) Tsuji, K.; Tomita, O.; Higashi, M.; Abe, R., Manganese-Substituted Polyoxometalate as an Effective Shuttle Redox Mediator in Z-Scheme Water Splitting under Visible Light. *ChemSusChem* **2016,** *9*, 2201-2208.

(15) Ettedgui, J.; Diskin-Posner, Y.; Weiner, L.; Neumann, R., Photoreduction of Carbon Dioxide to Carbon Monoxide with Hydrogen Catalyzed by a Rhenium(I) Phenanthroline-Polyoxometalate Hybrid Complex. *J. Am. Chem. Soc.* **2011,** *133*, 188-190.

(16) Ci, C. G.; Carbo, J. J.; Neumann, R.; de Graaf, C.; Poblet, J. M., Photoreduction Mechanism of CO_2 to CO Catalyzed by a Rhenium(I)- Polyoxometalate Hybrid Compound. *ACS Catal.* **2016,** *6*, 6422-6428.

(17) Proust, A.; Matt, B.; Villanneau, R.; Guillemot, G.; Gouzerh, P.; Izzet, G., Functionalization and Post-Functionalization: a Step towards Polyoxometalate-Based Materials. *Chem. Soc. Rev.* **2012,** *41*, 7605-7622.

(18) Izzet, G.; Volatron, F.; Proust, A., Tailor-made Covalent Organic-Inorganic Polyoxometalate Hybrids: Versatile Platforms for the Elaboration of Functional Molecular Architectures. *Chem. Rec.* **2017,** *17*, 250-266.

(19) Laurans, M.; Trinh, K.; Dalla Francesca, K.; Izzet, G.; Humblot, V.; Alvez, S.; Pluchery, O.; Vuillaume, D.; Lenfant, S.; Volatron, F.; Proust, A., Covalent Grafting of Polyoxometalate Hybrids onto Flat Silicon Oxide: a Step Forward on the Control of POMs Layers on Oxides. *to be submitted*.

(20) Rinfray, C.; Izzet, G.; Pinson, J.; Derouich, S. G.; Ganem, J. J.; Combellas, C.; Kanoufi, F.; Proust, A., Electrografting of Diazonium-Functionalized Polyoxometalates: Synthesis,

Immobilisation and Electron-Transfer Characterisation from Glassy Carbon. *Chem.-Eur. J.* **2013,** *19*, 13838-13846.

(21) Laurans, M.; Francesca, K. D.; Volatron, F.; Izzet, G.; Guerin, D.; Vuillaume, D.; Lenfant, S.; Proust, A., Molecular Signature of Polyoxometalates in Electron Transport of Silicon-based Molecular Junctions. *Nanoscale* **2018,** *10*, 17156-17165.

(22) Massin, J.; Brautigam, M.; Kaeffer, N.; Queyriaux, N.; Field, M. J.; Schacher, F. H.; Popp, J.; Chavarot-Kerlidou, M.; Dietzek, B.; Artero, V., Dye-sensitized PS-b-P2VP-Templated Nickel Oxide Films for Photoelectrochemical Applications. *Interface Focus* **2015,** *5*: 20140083.

(23) Kaeffer, N.; Massin, J.; Lebrun, C.; Renault, O.; Chavarot-Kerlidou, M.; Artero, V., Covalent Design for Dye-Sensitized H-2-Evolving Photocathodes Based on a Cobalt Diimine-Dioxime Catalyst. *J. Am. Chem. Soc.* **2016,** *138*, 12308-12311.

(24) Massin, J.; Brautigam, M.; Bold, S.; Wachtler, M.; Pavone, M.; Munoz-Garcia, A. B.; Dietzek, B.; Artero, V.; Chavarot-Kerlidou, M., Investigating Light-Driven Hole Injection and Hydrogen Evolution Catalysis at Dye-Sensitized NiO Photocathodes: A Combined Experimental-Theoretical Study. *J. Phys. Chem. C* **2019,** *123*, 17176-17184.

(25) Brennan, B. J.; Durrell, A. C.; Koepf, M.; Crabtree, R. H.; Brudvig, G. W., Towards Multielectron Photocatalysis: a Porphyrin Array for Lateral Hole Transfer and Capture on a Metal Oxide Surface. *Phys. Chem. Chem. Phys.* **2015,** *17*, 12728-12734.

(26) Hoertz, P. G.; Chen, Z. F.; Kent, C. A.; Meyer, T. J., Application of High Surface Area Tin-Doped Indium Oxide Nanoparticle Films as Transparent Conducting Electrodes. *Inorg. Chem.* **2010,** *49*, 8179-8181.

(27) Sung, W. L.; An, B. W.; Qi, B.; Liu, T.; Jin, M.; Duan, C. Y., Dual-Excitation Polyoxometalate-Based Frameworks for One-Pot Light-Driven Hydrogen Evolution and Oxidative Dehydrogenation. *ACS Appl. Mater. Interfaces* **2018,** *10*, 13462-13469.

(28) El Moll, H.; Black, F. A.; Wood, C. J.; Al-Yasari, A.; Marri, A. R.; Sazanovich, I. V.; Gibson, E. A.; Fielden, J., Increasing p-Type Dye Sensitised Solar Cell Photovoltages using Polyoxometalates. *Phys. Chem. Chem. Phys.* **2017,** *19*, 18831-18835.

(29) Ahmed, I.; Farha, R.; Goldmann, M.; Ruhlmann, L., A Molecular Photovoltaic System Based on Dawson Pype Polyoxometalate and Porphyrin Formed by Layer-by-Layer Self Assembly. *Chem. Commun.* **2013,** *49*, 496-498.

(30) Chen, L.; Chen, W. L.; Wang, X. L.; Li, Y. G.; Su, Z. M.; Wang, E. B., Polyoxometalates in Dye-Sensitized Solar Cells. *Chem. Soc. Rev.* **2019,** *48*, 260-284.